

Supplementary Information

Vertebrate Cryptochromes are Vestigial Flavoproteins

Roger J. Kutta,^{1,2*} Nataliya Archipowa,¹ Linus O. Johannissen,¹ Alex R. Jones,^{1,2*} and Nigel S. Scrutton^{1*}

1. Manchester Institute of Biotechnology (MIB) and School of Chemistry, The University of Manchester, 131 Princess Street, Manchester, M1 7DN, UK.

2. Photon Science Institute and School of Chemistry, The University of Manchester, Alan Turing Building, Oxford Road, Manchester, M13 9PL, UK.

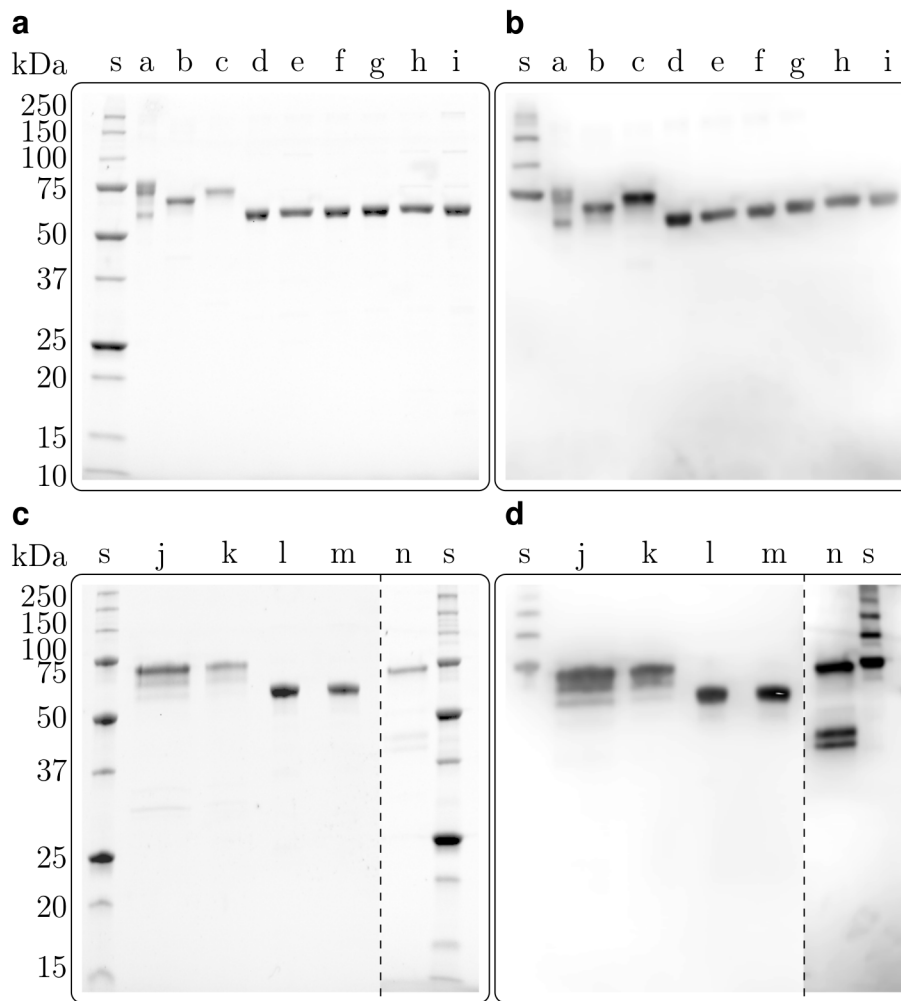


Figure S1. SDS-PAGE and Western blot analysis of purified CRY proteins. **a** and **c**: SDS-PAGE of Marker (s; Precision Plus Protein™ Unstained Standards, BioRad), SbCRY1a (a), HsCRY1 (b), HsCRY2 (c), DmCRY (d), DmCRY-R237E (e), DmCRY-R298E (f), DmCRY-Q311E (g), DmCRY-R237E-R298E (h), DmCRY-R298E-Q311E (i), HsCRY2-H243R (j), HsCRY2-S415N (k), DmCRY-R237H (l), DmCRY-N419S (m), and HsCRY2-H243R-S415N (n). **b** and **d**: Corresponding Western blot of **a** and **c**. The multiple bands in lanes (a), (j) and (k) indicate some minor degradation of the protein. Selected proteins (the first four marker bands) in the commercial strep-tag marker sample also cross-react with anti-His antibodies used in panels **b** and **d**. The dashed lines in panels **c** and **d** indicate the junctions between two individual gels/blots.

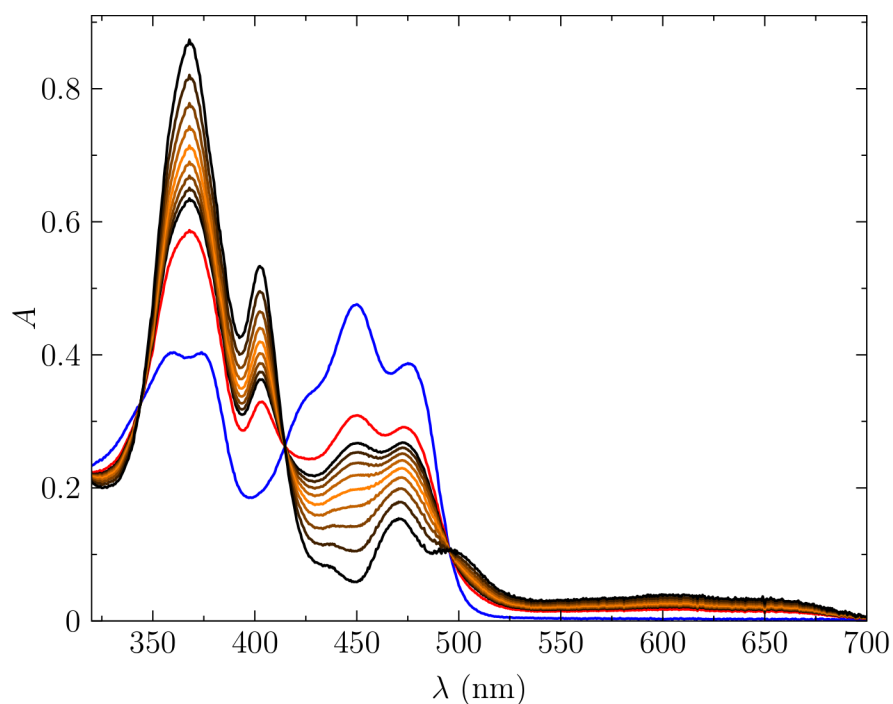


Figure S2. Determination of the pure FAD radical anion spectrum in DmCRY *via in silico* titration. The absorption spectra of DmCRY were recorded before (blue line) and directly after illumination with a 1 s blue-light pulse (red line). The spectrum of the pure FAD radical anion was generated by subtracting the spectrum of the oxidized FAD from the spectrum after blue-light illumination until the signatures of the spectrum of the oxidized FAD disappeared. The spectral sequence from black to orange to black corresponds to contributions of the oxidized spectrum of 20% to 60% in 5% steps, respectively.

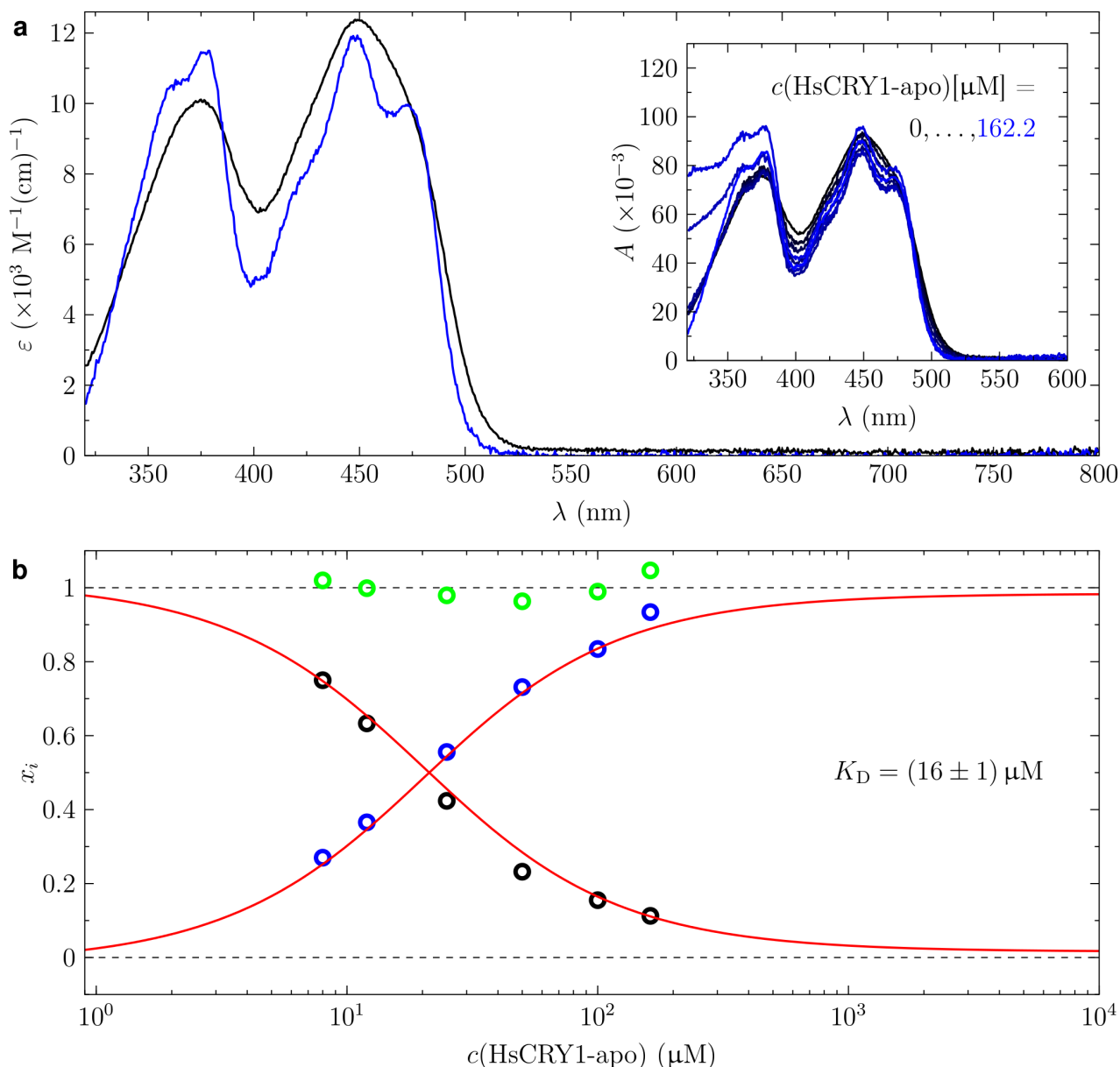


Figure S3. Determination of the FAD-binding affinity in HsCRY1. **a:** pure UV-visible absorption spectra of unbound FAD (black) and bound in HsCRY1 (blue) extracted from the raw data (inset in panel **a**: raw data minus fitted scatter contribution) as described in the Materials and Methods section of the main text. **b:** mole fractions of unbound FAD (black open circles) and bound in HsCRY1 (blue open circles) as determined from fitting the pure spectra from panel **a** to each spectrum of the inset in panel **a** correlated with the HsCRY1-apo concentration. The green open circles represent the sum of the mole fractions. The red lines represent the global fits of the binding equation 4 to the data.

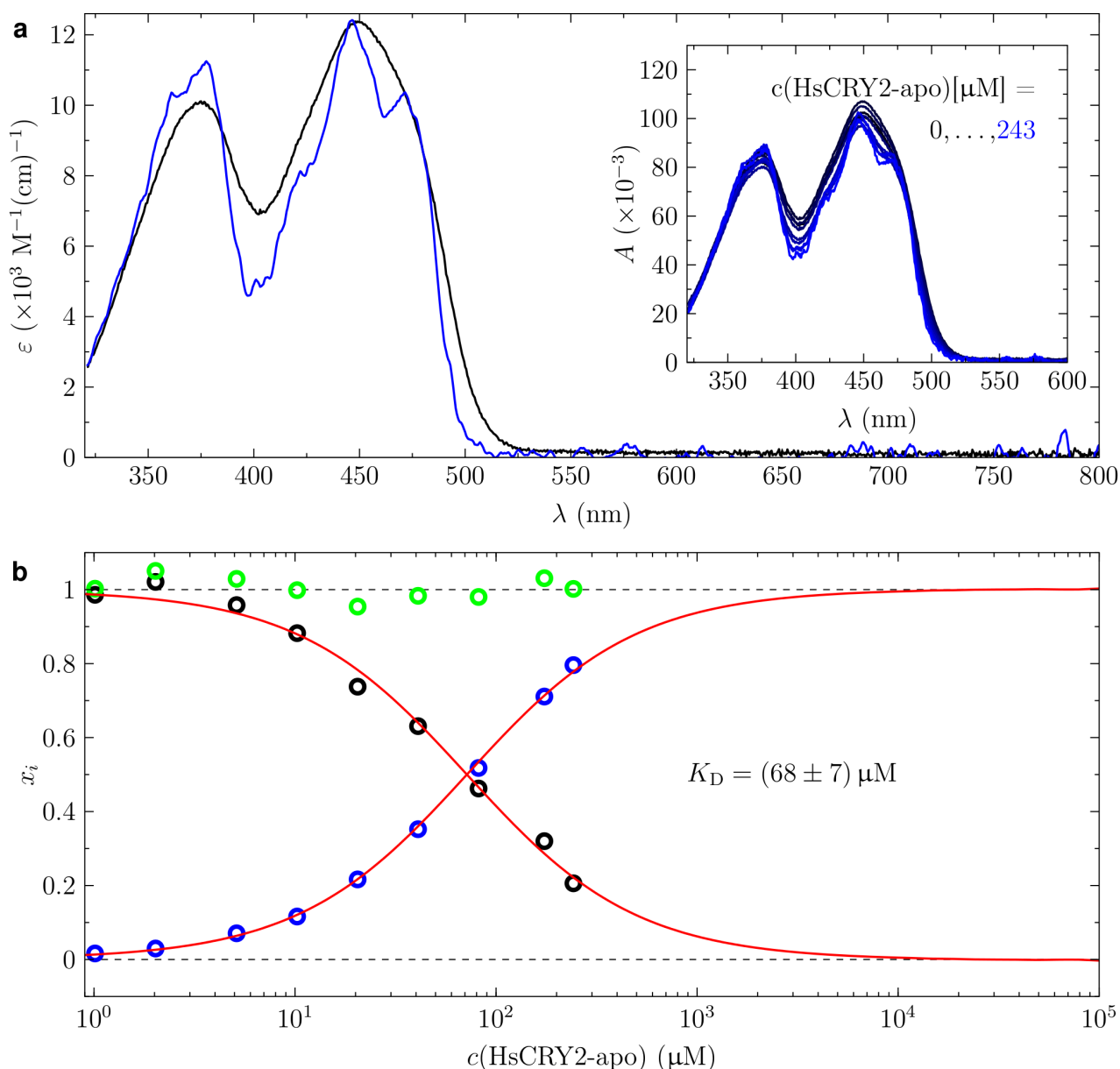


Figure S4. Determination of the FAD-binding affinity in HsCRY2. **a:** pure UV-visible absorption spectra of unbound FAD (black) and bound in HsCRY2 (blue) extracted from the raw data (inset in panel **a**: raw data minus fitted scatter contribution) as described in the Materials and Methods section of the main text. **b:** mole fractions of unbound FAD (black open circles) and bound in HsCRY2 (blue open circles) as determined from fitting the pure spectra from panel **a** to each spectrum of the inset in panel **a** correlated with the HsCRY2-apo concentration. The green open circles represent the sum of the mole fractions. The red lines represent the global fits of the binding equation 4 to the data.

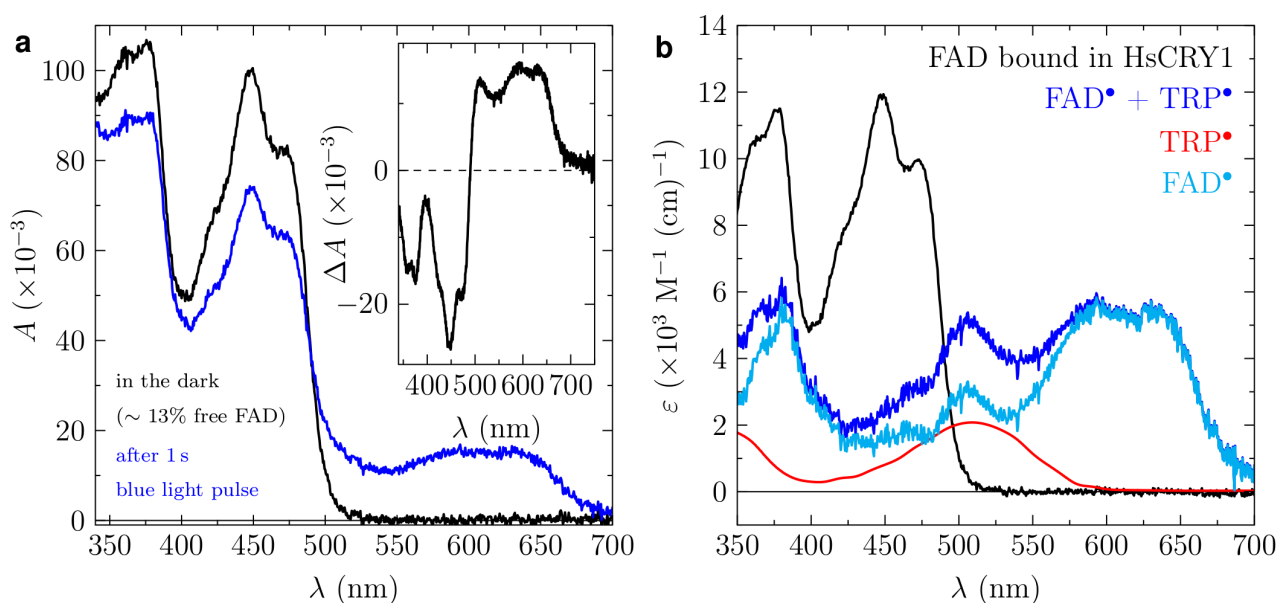


Figure S5. Determination of the pure neutral FAD radical spectrum and the counter neutral tryptophan radical in HsCRY1 via *in silico* titration. Absorption spectra of a sample containing 8 μM FAD and *ca.* 100 μM HsCRY1 before (black line in panel **a**) and directly after illumination with a 1 s blue-light pulse (blue line in panel **a**). Since this sample still contained *ca.* 13% of unbound FAD, the difference spectrum (inset in panel **a**) subtracts the contribution of unbound FAD. Adding the pure spectrum of fully bound FAD to HsCRY1 from Figure S3a to the difference spectrum in such a way that its characteristic fine structural features disappear, results in a spectrum (blue line in panel **b**) with a high similarity to known spectra for the neutral flavin semiquinone radical, *e.g.* shown in^{1,2}. However, some deviations can still be seen especially in the range between 450 to 550 nm. These deviations can be explained by the contributions of the neutral tryptophan radical (red line extracted from³). By subtracting a certain amount of the neutral tryptophan radical from the mixture spectrum it is possible to obtain a perfect match to the known flavin neutral radical spectrum (cyan line). (A detailed time-resolved analysis of the mechanism including branching ratios, the photoproduct, and a discussion about the proton donor is beyond the scope of this work and will be presented elsewhere.)

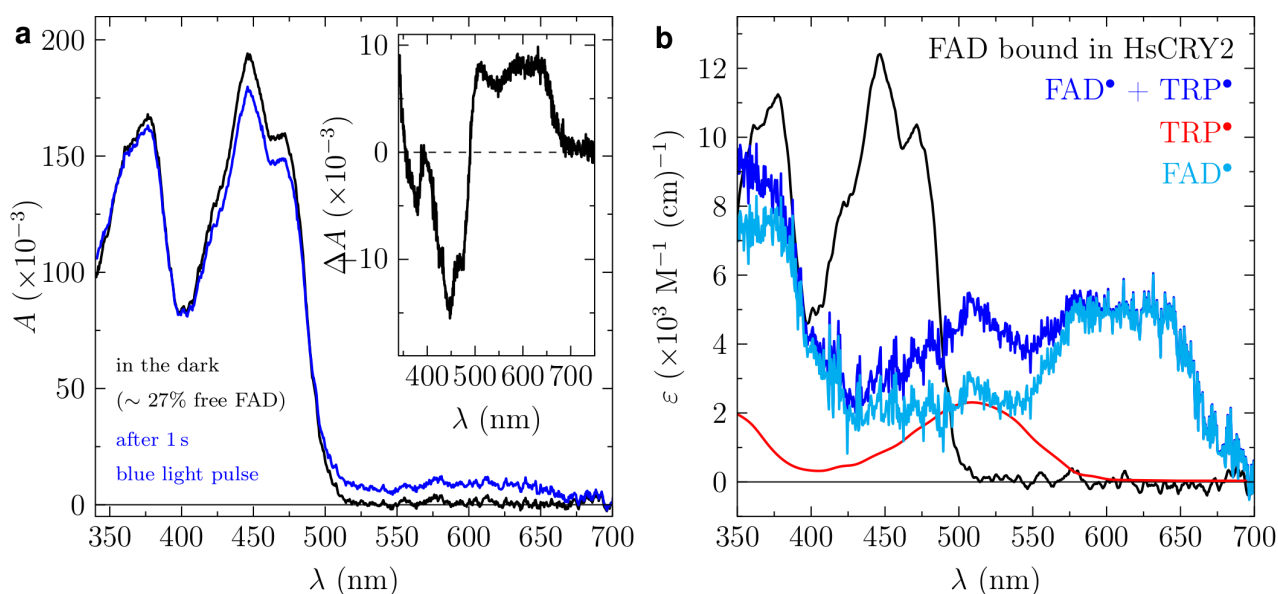


Figure S6. Determination of the pure neutral FAD radical spectrum and the counter neutral tryptophan radical in HsCRY2 via *in silico* titration. Absorption spectra of a sample containing 15.4 μM FAD and *ca.* 317 μM HsCRY2 before (black line in panel **a**) and directly after illumination with a 1 s blue-light pulse (blue line in panel **a**). Since this sample still contained *ca.* 27% of unbound FAD, the difference spectrum (inset in panel **a**) subtracts the contribution of unbound FAD. Adding the pure spectrum of fully bound FAD to HsCRY2 from Figure S4a to the difference spectrum in such a way that its characteristic fine structural features disappear, results in a spectrum (blue line in panel **b**) with a high similarity to known spectra for the neutral flavin semiquinone radical, *e.g.* shown in^{1,2}. However, some deviations can still be seen especially in the range between 450 to 550 nm. These deviations can be explained by the contributions of the neutral tryptophan radical (red line extracted from³). By subtracting a certain amount of the neutral tryptophan radical from the mixture spectrum it is possible to obtain a perfect match to the known flavin neutral radical spectrum (cyan line). (A detailed time-resolved analysis of the mechanism including branching ratios, the photoproduct, and a discussion about the proton donor is beyond the scope of this work and will be presented elsewhere.)

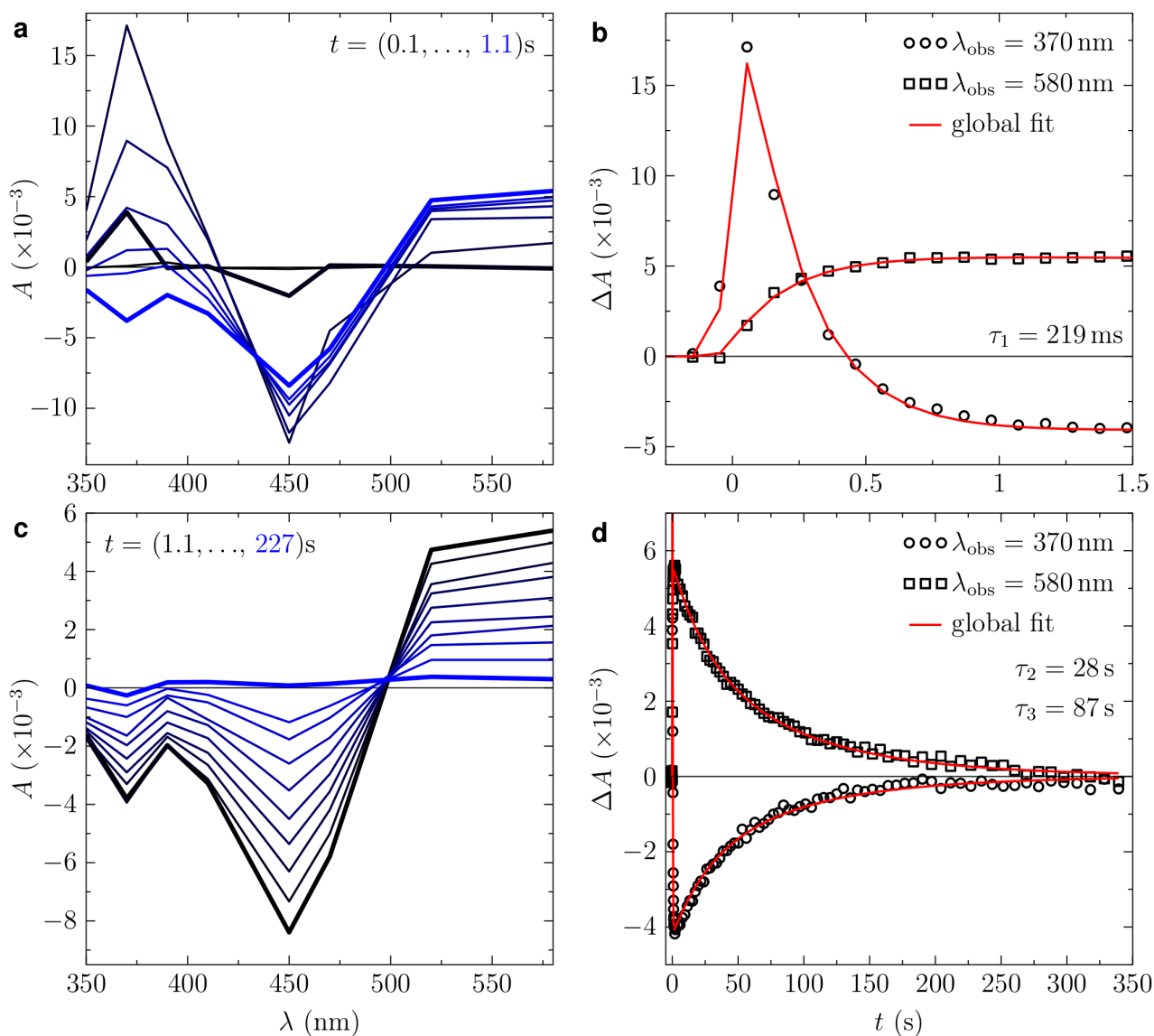


Figure S7. Photo-induced formation and decay of the neutral FAD semiquinone radical bound in HsCRY1. UV-visible absorption changes at single wavelengths in the range from 350 to 580 nm induced by single 100 ms blue-light pulse were recorded for a sample containing 8 μM FAD and *ca.* 100 μM HsCRY1. The spectrally (a and c) and temporally (b and d) resolved UV-visible absorption changes up to 1 s (a and b) and 350 s (c and d) are shown at two selected wavelength representative for the main features of the anionic (370 nm) and neutral (580 nm) FAD semiquinone radicals. The red lines represent the global fit of two exponential functions to the entire data matrix with the lifetimes of 219 ms, 28 s and 87 s. (A detailed time-resolved analysis of the mechanism including branching ratios, the photoproduct, and a discussion about the proton donor is beyond the scope of this work and will be presented elsewhere.)

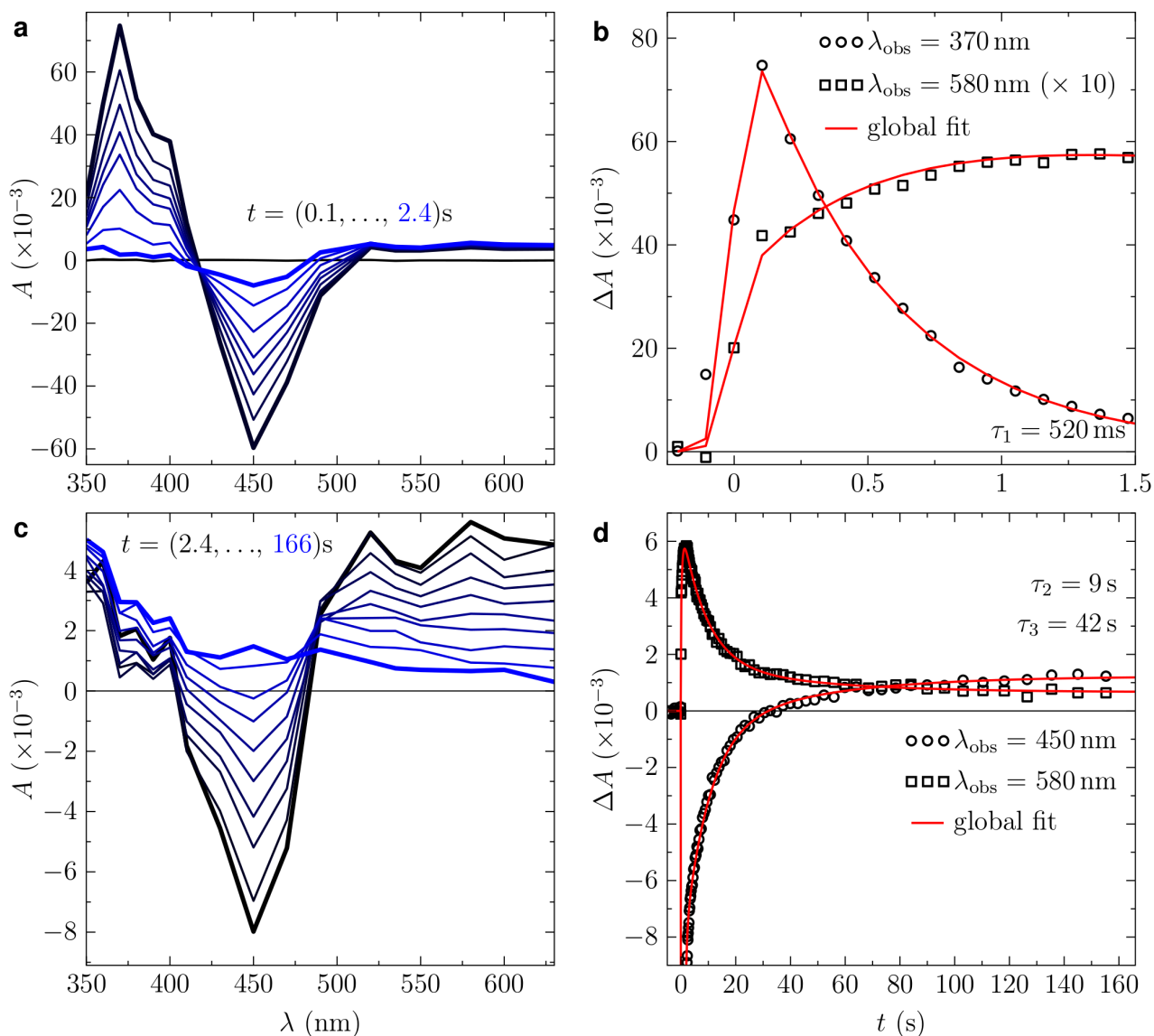


Figure S8. Photo-induced formation and decay of the neutral FAD semiquinone radical bound in HsCRY2. UV-visible absorption changes at single wavelengths in the range from 350 to 580 nm induced by single 100 ms blue-light pulse were recorded for a sample containing 15.4 μM FAD and *ca.* 317 μM HsCRY2. The spectrally (a and c) and temporally (b and d) resolved UV-visible absorption changes up to 1 s (a and b) and 350 s (c and d) are shown at three selected wavelength representative for the main features of the anionic (370 nm), the neutral (580 nm) FAD semiquinone radicals, and the oxidized FAD. The red lines represent the global fit of two exponential functions to the entire data matrix with the lifetimes of 520 ms, 9 s, and 42 s. (A detailed time-resolved analysis of the mechanism including branching ratios, the photoproduct, and a discussion about the proton donor is beyond the scope of this work and will be presented elsewhere.)

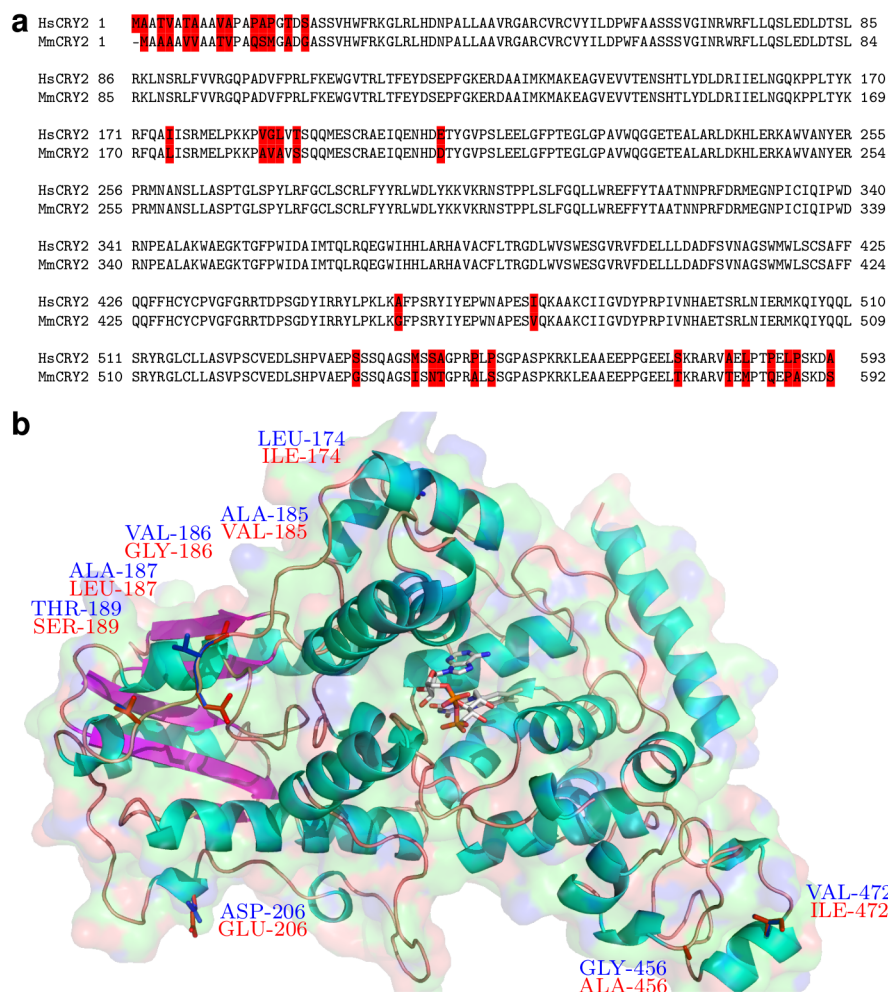


Figure S9. Structure and sequence alignment between HsCRY2 and MmCRY2. **a:** Sequence alignment. The differing amino acids between HsCRY2 and MmCRY2 are highlighted with a red background. **b:** Structural alignment. HsCRY2 is a homology model based on the template structure from MmCRY2 (yellow, PDB code: 4I6G); all secondary elements are therefore identical and only the resolved amino acids could be modelled. All differing amino acids as well as the FAD are shown as stick representation.

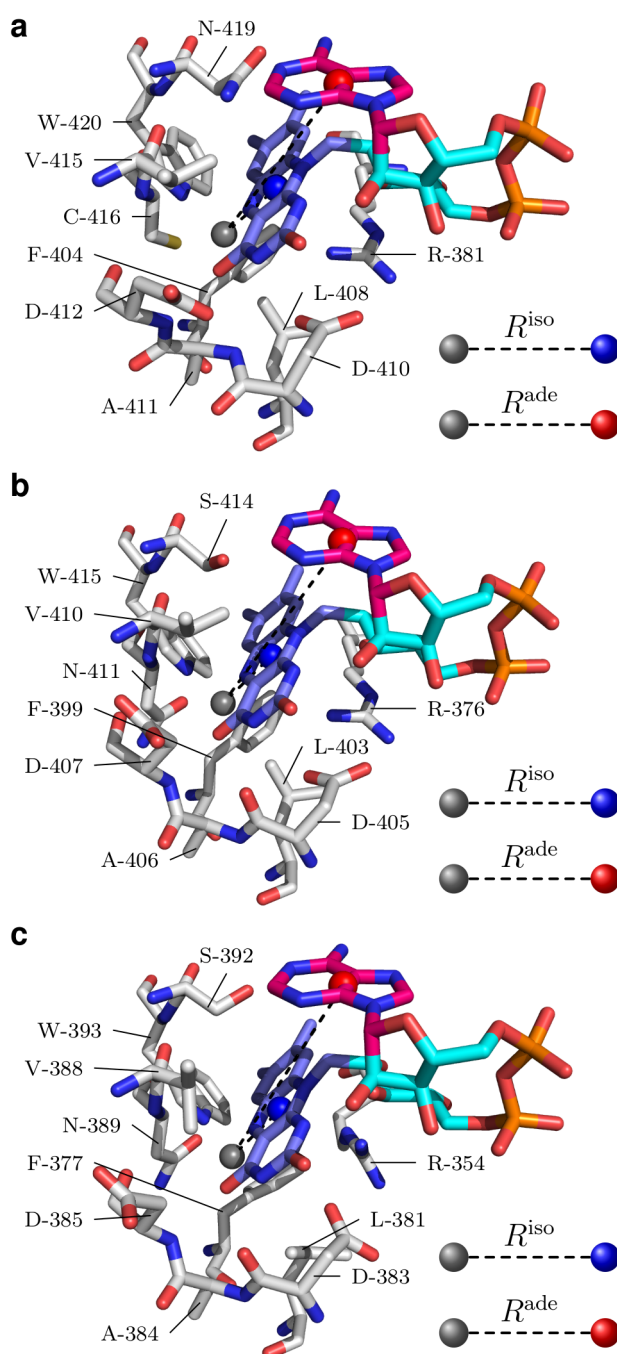


Figure S10. Definition of collective variables (CVs) used in metadynamics simulations. R^{iso} is defined as the centre-of-mass from the isoalloxazine (blue sphere) to the centre-of-mass of amino acid residues (gray sphere) and R^{ade} as the centre-of-mass from the adenine moiety (red sphere) to the same centre-of-mass of amino acid residues (gray spheres) involved in FAD-binding as represented. **a:** DmCRY. **b:** MmCRY2. **c:** SbCRY1a.

HsCRY2/1-593	1	-----MAATVATAA VAPAPAGTDSASSVHWFRKGLRLHNDPALAAVRG-----	ARCVRVYILD PWF AASSVGINRWRLQLSQLEDLDTSL	85
MmCRY2/1-592	1	-----MAAAAVVAAATVPAQSMGADGASSVHWFRKGLRLHNDPALAAVRG-----	ARCVRVYILD PWF AASSVGINRWRLQLSQLEDLDTSL	84
GgCRY2/1-582	1	-----MAAAASPPRG-----	AASLRVYILD PWF AASSVGINRWRLQLSQLEDLDTSL	75
HsCRY1/1-586	1	-----MGVNAVHWFRKGLRLHNDPALKECIQG-----	ADTIRCVYILD PWF AGSSNVGINRWRLQLSQLEDLDTSL	66
MmCRY1/1-606	1	-----MGVNAVHWFRKGLRLHNDPALKECIQG-----	ADTIRCVYILD PWF AGSSNVGINRWRLQLSQLEDLDTSL	66
ErCRY1/1-620	1	-----MGVNAVHWFRKGLRLHNDPALRECIRG-----	ADTVRCVYILD PWF AGSSNVGINRWRLQLSQLEDLDTSL	66
SbCRY1/1-620	1	-----MGVNAVHWFRKGLRLHNDPALRECIRG-----	ADTVRCVYILD PWF AGSSNVGINRWRLQLSQLEDLDTSL	66
GgCRY1/1-621	1	-----MGVNAVHWFRKGLRLHNDPALRECIRG-----	ADTVRCVYILD PWF AGSSNVGINRWRLQLSQLEDLDTSL	66
DpCRY2/1-742	1	MSVAETLPLRARSPTAQKSSQAGVPKEKHTVHWFRKGLRLHNDPALREGIIVD-----	ATTFRCVYILD PWF AASSNVGINRWRLQLSQLEDLDTSL	92
MbCRY1/1-548	1	-----MLGGSVLVFRHGLRLHNDPNSLSHALE-----	EKGFPFFPVIFDGETAGTKLVGYNRMRYLLEALDLDLQK	67
HaCRY1/1-528	1	-----MLGGSVLVFRHGLRLHNDPNSLSHALE-----	EKGFPFFPVIFDGETAGTKLVGYNRMRYLLEALDLDLQK	67
BmCRY1/1-536	1	-----MLGGSVLVFRHGLRLHNDPNSLSHALE-----	ETSGPFFPVIFDGETAGTKLVGYNRMRYLLEALDLDLQK	67
DpCRY1/1-534	1	-----MLGGNVIVFRHGLRLHNDPNSLSHALE-----	DASSPFFPVIFDGETAGTKLVGYNRMRYLLEALDLDLQK	67
DmCRY1/1-542	1	-----MATRGANVIFRHLGLRLHNDPALAALAD-----	KDQGIALLPVIFDGETAGTKLVGYNRMRYLLEALDLDLQK	71
NbCRY1/1-542	1	-----MSLNIIIFRHLGLRLHNDPALDAISD-----	KDEGIALLPVIFDGETAGTKLVGYNRMRYLLEALDLDLQK	68
AgCRY1/1-545	1	-----MTNNILVFRHGLRLHNDPNSLSHALEKSDCVNQSSAEVKLFPIIFDGETAGTRIVGYNRMRYLLEALDLDLQK	74	
HsCRY2/1-593	86	RKLN---SRLFVIRGQPADVPRLFKWGVTRITFEYDESEPFKGERDAAIKMAKEAGVEVVTENSHITLYDLDRITELNGQKPLTYKRQALISRMELP	182	
MmCRY2/1-592	85	RKLN---SRLFVIRGQPADVPRLFKWGVTRITFEYDESEPFKGERDAAIKMAKEAGVEVVTENSHITLYDLDRITELNGQKPLTYKRQALISRMELP	181	
GgCRY2/1-582	76	RKLN---SRLFVIRGQPADVPRLFKWGVTRITFEYDESEPFKGERDAAIKMAKEAGVEVVTENSHITLYDLDRITELNGQKPLTYKRQALISRMELP	172	
HaCRY1/1-586	67	RKLN---SRLFVIRGQPADVPRLFKWGVTRITFEYDESEPFKGERDAAIKMAKEAGVEVVTENSHITLYDLDRITELNGQKPLTYKRQALISRMELP	163	
MmCRY1/1-606	67	RKLN---SRLFVIRGQPADVPRLFKWGVTRITFEYDESEPFKGERDAAIKMAKEAGVEVVTENSHITLYDLDRITELNGQKPLTYKRQALISRMELP	163	
ErCRY1/1-620	67	RKLN---SRLFVIRGQPADVPRLFKWGVTRITFEYDESEPFKGERDAAIKMAKEAGVEVVTENSHITLYDLDRITELNGQKPLTYKRQALISRMELP	163	
SbCRY1/1-620	67	RKLN---SRLFVIRGQPADVPRLFKWGVTRITFEYDESEPFKGERDAAIKMAKEAGVEVVTENSHITLYDLDRITELNGQKPLTYKRQALISRMELP	163	
GgCRY1/1-621	67	RKLN---SRLFVIRGQPADVPRLFKWGVTRITFEYDESEPFKGERDAAIKMAKEAGVEVVTENSHITLYDLDRITELNGQKPLTYKRQALISRMELP	163	
DpCRY2/1-742	93	RKLN---SRLFVIRGQPADVPRLFKWGVTRITFEYDESEPFKGERDAAIKMAKEAGVEVVTENSHITLYDLDRITELNGQKPLTYKRQALISRMELP	189	
MbCRY1/1-548	68	KKHG---GRLLIMIKGKPNVFRRLWEEFGIRLCEFDQCEPVRARDDSVKSAKEIGVVCREHVSHTLWEPDVIKANGGIPPLTYQMLHTVATTGDP	164	
HaCRY1/1-528	68	KKFG---GRLLIMIKGKPNVFRRLWEEFGIRLCEFDQCEPVRARDDSVKSAKEIGVVCREHVSHTLWEPDVIKANGGIPPLTYQMLHTVATTGDP	164	
BmCRY1/1-536	68	KKYG---GRLLIMIKGKPNVFRRLWEEFGIRLCEFDQCEPVRARDDSVKSAKEIGVVCREHVSHTLWEPDVIKANGGIPPLTYQMLHTVATTGDP	164	
DpCRY1/1-534	68	KKYG---GRLLIMIKGKPNVFRRLWEEFGIRLCEFDQCEPVRARDDSVKSAKEIGVVCREHVSHTLWEPDVIKANGGIPPLTYQMLHTVATTGDP	164	
DmCRY1/1-542	72	QAATDGRGRLLVFEQGPAYIFRRLHEQVRLHRCIDQCEPVRARDDSVKSAKEIGVVCREHVSHTLWEPDVIKANGGIPPLTYQMLHTVATTGDP	171	
NbCRY1/1-542	69	RSVSLSLGRLLVFEQGPAYIFRRLHEQVRLHRCIDQCEPVRARDDSVKSAKEIGVVCREHVSHTLWEPDVIKANGGIPPLTYQMLHTVATTGDP	168	
AgCRY1/1-545	75	RDLG---GQLLVFRQDSVTVLRRLFEELNIKKLCYEDQCEPVRARDDSVKSAKEIGVVCREHVSHTLWEPDVIKANGGIPPLTYQMLHTVATTGDP	171	
HsCRY2/1-593	183	KKPVGLVTSQQMESCRATQENHDDTYG-----	VPSLEELGFPTD---GLGPAVWGGETEALRLDKHL---ERKAWVANFERPRMANS	262
MmCRY2/1-592	182	KKPAVASVQQMESCRATQENHDDTYG-----	VPSLEELGFPTD---GLGPAVWGGETEALRLDKHL---ERKAWVANFERPRMANS	261
GgCRY2/1-582	173	KKPVSSIVSQMTECKVDIQENHDDTYG-----	VPSLEELGFPTD---GLGPAVWGGETEALRLDKHL---ERKAWVANFERPRMANS	252
HaCRY1/1-586	164	ETPVETITSEVIEKCTTPVSDHDEKYG-----	VPSLEELGFPTD---GLSSAVWPGGETEALTRLERHL---ERKAWVANFERPRMANS	243
MmCRY1/1-606	164	EMPADTITSDVICKMCTPLSDHDEKYG-----	VPSLEELGFPTD---GLSSAVWPGGETEALTRLERHL---ERKAWVANFERPRMANS	243
ErCRY1/1-620	164	EMPVETITPEVMKCTTPVSDHDEKYG-----	VPSLEELGFPTD---GLPSAVWPGGETEALTRLERHL---ERKAWVANFERPRMANS	243
SbCRY1/1-620	164	EMPVETITPEVMKCTTPVSDHDEKYG-----	VPSLEELGFPTD---GLPSAVWPGGETEALTRLERHL---ERKAWVANFERPRMANS	243
GgCRY1/1-621	164	EMPVETITPEVMKCTTPVSDHDEKYG-----	VPSLEELGFPTD---GLPSAVWPGGETEALTRLERHL---ERKAWVANFERPRMANS	243
DpCRY2/1-742	190	PSAETPISLETNRAVPTISDNHDERFG-----	VPTLEELGFPTD---GLKPPITIGGNEALLRLERHL---ERKAWVANFERPRMANS	269
MbCRY1/1-548	165	PRPVSIDT-----	DFTGVKFGSLPESFYHEFTVYDKTPKPEDLVGFLE---NEDIRMRIRVGGETTAALKMQQRLLAVEYETFLRGSYLPHTGNPD	250
HaCRY1/1-528	165	PRPVPNI-----	DFTGVKFGSLPESFYHEFTVYDKTPKPEDLVGFLE---NEDIRMRIRVGGETTAALKMQQRLLAVEYETFLRGSYLPHTGNPD	250
BmCRY1/1-536	165	PRPVDNA-----	KLKGIKFGTLPLCFYEEFTVYDKTPKPEDLVGFLE---NEDIRMRIRVGGETTAALKMQQRLLAVEYETFLRGSYLPHTGNPD	250
DpCRY1/1-534	165	PRPVDNV-----	DLNGVNFVGLPESFYHEFTVYDKTPKPEDLVGFLE---NEDIRMRIRVGGETTAALKMQQRLLAVEYETFLRGSYLPHTGNPD	250
DmCRY1/1-542	172	PRPTADA-----	RLEDATFVELDPEFCRSKLKLEQLTPEHFNVYGDNGMFLAKINRGCEQALLLDERLKVEQHAFERGFYLPNQALPN	258
NbCRY1/1-542	169	PRPVPDP-----	DHNKVKFVLSKLKIDLVGFLESTPEDFSVYDPSLSYLAKVKVIGGETQALLHLDQRKVEESAFKCYGLPNQAKPN	255
AgCRY1/1-545	172	PRPVGAP-----	NFEYVEFGVFPALLASELKLQCMQAPDDFGTHYDGNARITAFQKIGGETRALLEALGARLKQEEAFREGYLPYTPQAKPE	258
HsCRY2/1-593	263	LLASPTGLSPYLRFGLSCLRLFYFRLDLYKKVKNSTPPSL-----	LFQQLWREFFYYTAATNNPRFDRMEGNPICQIPWDR---NPEALAKWAEGR	354
MmCRY2/1-592	262	LLASPTGLSPYLRFGLSCLRLFYFRLDLYKKVKNSTPPSL-----	LFQQLWREFFYYTAATNNPRFDRMEGNPICQIPWDR---NPEALAKWAEGR	353
GgCRY2/1-582	253	LLASPTGLSPYLRFGLSCLRLFYFRLDLYKKVKNSTPPSL-----	LYQQLWREFFYYTAATNNPRFDRMEGNPICQIPWDR---NPEALAKWAEGR	344
HaCRY1/1-586	244	LLASPTGLSPYLRFGLSCLRLFYFRLDLYKKVKNSTPPSL-----	LYQQLWREFFYYTAATNNPRFDRMEGNPICQIPWDR---NPEALAKWAEGR	335
MmCRY1/1-606	244	LLASPTGLSPYLRFGLSCLRLFYFRLDLYKKVKNSTPPSL-----	LYQQLWREFFYYTAATNNPRFDRMEGNPICQIPWDR---NPEALAKWAEGR	335
ErCRY1/1-620	244	LLASPTGLSPYLRFGLSCLRLFYFRLDLYKKVKNSTPPSL-----	LYQQLWREFFYYTAATNNPRFDRMEGNPICQIPWDR---NPEALAKWAEGR	335
SbCRY1/1-620	244	LLASPTGLSPYLRFGLSCLRLFYFRLDLYKKVKNSTPPSL-----	LYQQLWREFFYYTAATNNPRFDRMEGNPICQIPWDR---NPEALAKWAEGR	335
GgCRY1/1-621	244	LLASPTGLSPYLRFGLSCLRLFYFRLDLYKKVKNSTPPSL-----	LYQQLWREFFYYTAATNNPRFDRMEGNPICQIPWDR---NPEALAKWAEGR	335
DpCRY2/1-742	270	LLSSQTGLSPYLRFGLSCLRLFYFRLDLYKKVKNSTPPSL-----	LHQQILWREFFYYCAATNNPRFDRMEGNPICQIPWDR---NPEALAKWAEGR	360
MbCRY1/1-548	251	LLGPPIISLSPALRFGLSVRFYFWSLQDLFQQVHQQ-----	RLATQSASHFITGQLIWREYFYTMSVNNPNYQMGAGNPICLDIPWKEPEGDELQRAVEGR	347
HaCRY1/1-528	251	LLGPPIISLSPALRFGLSVRFYFWSLQDLFQQVHQQ-----	RLATQSASHFITGQLIWREYFYTMSVNNPNYQMGAGNPICLDIPWKEPEGDELQRAVEGR	347
BmCRY1/1-536	251	LLGPPIISLSPALRFGLSVRFYFWSLQDLFQQVHQQ-----	SLCS---TQYITGQLIWREYFYTMSVNNPNYQMGAGNPICLDIPWKEPEGDELQRAVEGR	344
DpCRY1/1-534	251	LLGPPIISLSPALRFGLSVRFYFWSLQDLFQQVHQQ-----	RLAS---TQYITGQLIWREYFYTMSVNNPNYQMGAGNPICLDIPWKEPEGDELQRAVEGR	344
DmCRY1/1-542	259	IHDSPKMSAHLRFGLSVRFYFWSLQDLFQQVHQQ-----	QLACVGRVGMQGAHITGQLIWREYFYTMSVNNPNYQMGAGNPICLDIPWKEPEGDELQRAVEGR	358
NbCRY1/1-542	256	ILSPKMSAHLRFGLSVRFYFWSLQDLFQQVHQQ-----	QLACVGRVGMQGAHITGQLIWREYFYTMSVNNPNYQMGAGNPICLDIPWKEPEGDELQRAVEGR	355
AgCRY1/1-545	259	ILGPATMSAHLRFGLSVRFYFWSLQDLFQQVHQQ-----	YPGHHITGQLIWREYFYTMSVNNPNYQMGAGNPICLDIPWKEPEGDELQRAVEGR	355

Figure S11. Sequence alignment of Type I and Type II CRY (part 1).

HeCRY2/1-593	355	GFFWIDAIMTQLRQEGWIHHLARHAVACFLTRGDLWISWESGVRVFEDELLDADFVSNAGSWMLSCSAFFQFFH--CYCPVGFGRRTDPSGDYIRRYL	452
MmCRY2/1-592	354	GFFWIDAIMTQLRQEGWIHHLARHAVACFLTRGDLWISWESGVRVFEDELLDADFVSNAGSWMLSCSAFFQFFH--CYCPVGFGRRTDPSGDYIRRYL	451
GgCRY2/1-582	345	GFFWIDAIMTQLRQEGWIHHLARHAVACFLTRGDLWISWESGVRVFEDELLDADFVSNAGSWMLSCSAFFQFFH--CYCPVGFGRRTDPSGDYIRRYL	442
HeCRY1/1-586	336	GFFWIDAIMTQLRQEGWIHHLARHAVACFLTRGDLWISWEEGKMKVFEELLDDADWSINAGSWMLSCSFFQFFH--CYCPVGFGRRTDPNGDYIRRYL	433
MmCRY1/1-606	348	GFFWIDAIMTQLRQEGWIHHLARHAVACFLTRGDLWISWEEGKMKVFEELLDDADWSINAGSWMLSCSFFQFFH--CYCPVGFGRRTDPNGDYIRRYL	433
ErCRY1/1-620	336	GFFWIDAIMTQLRQEGWIHHLARHAVACFLTRGDLWISWEEGKMKVFEELLDDADWSINAGSWMLSCSFFQFFH--CYCPVGFGRRTDPNGDYIRRYL	433
SbCRY1/1-620	336	GFFWIDAIMTQLRQEGWIHHLARHAVACFLTRGDLWISWEEGKMKVFEELLDDADWSINAGSWMLSCSFFQFFH--CYCPVGFGRRTDPNGDYIRRYL	433
GgCRY1/1-621	336	GFFWIDAIMTQLRQEGWIHHLARHAVACFLTRGDLWISWEEGKMKVFEELLDDADWSINAGSWMLSCSFFQFFH--CYCPVGFGRRTDPNGDYIRRYL	433
DpCRY2/1-742	361	GFFWIDAIMIQLRNDGWIHHLARHAVACFLTRGDLWISWEEGKMKVFEELLDDADWSINAGSWMLSCSFFQFFH--CYCPVFRGRKTPDNGDFIRKI	458
MbCRY1/1-548	348	GFFFDVDAAMRQLRTEGLWHLHAARNTVASFLTRGTLWLSWEHGLNHFLKYLLDADWSVCAGNMMWVSSSAFEALLDSGECACPVLQRLDPSGEVRRYV	447
HaCRY1/1-528	348	GFFFDVDAAMRQLRTEGLWHLHAARNTVASFLTRGTLWLSWEHGLNHFLKYLLDADWSVCAGNMMWVSSSAFEALLDSGECACPVLQRLDPSGEVRRYV	447
BmCRY1/1-536	345	GFFFDVDAAMRQLRTEGLWHLHAARNTVASFLTRGTLWLSWEHGLNHFLKYLLDADWSVCAGNMMWVSSSAFEALLDSGECACPVLQRLDPSGEVRRYV	444
DpCRY1/1-534	345	GFFFDVDAAMRQLRTEGLWHLHAARNTVASFLTRGTLWLSWEHGLNHFLKYLLDADWSVCAGNMMWVSSSAFEALLDSGECACPVLQRLDPSGEVRRYV	444
DmCRY1/1-542	359	GFFLIDGAMRQLLAEGWLHHTLRNTVATFLTRGGLWQSWEHGLQHFLKYLLDADWSVCAGNMMWVSSSAFERLLDSSLVTCPVALAKRLDPDQYIKQV	458
NbCRY1/1-542	356	GFFLIDGAMRQLLAEGWLHHTLRNTVATFLTRGGLWQSWEHGLQHFLKYLLDADWSVCAGNMMWVSSSAFERLLDSSLVTCPVALAKRLDPDQYIKQV	455
AgCRY1/1-545	356	GFFMIDAMRQLLAEGWLHHTLRNTVATFLTRGGLWLSWEEGLQHFLKYLLDADWSVCAGNMMWVSSSAFERLLDSSKCTCIALAKRLDPKGDYVYRKL	455
HeCRY2/1-593	453	PKLKAFPSRYIYEPWNAPESIQKAACIIIGVDYPRPIVNHAEASRLNIERMKQIYQQLSRYRGLC-----LLASVPSC-----	525
MmCRY2/1-592	452	PKLKGFPSRYIYEPWNAPESVQKAACIIIGVDYPRPIVNHAEASRLNIERMKQIYQQLSRYRGLC-----LLASVPSC-----	524
GgCRY2/1-582	443	PKLKGFPSRYIYEPWNAPESVQKAACIIIGVDYPRPIVNHAEASRLNIERMKQIYQQLSRYRGLC-----LLASVPSC-----	515
HeCRY1/1-586	434	PVLRGFFAKYIYDPWNAPEGIQKAKCLIGVNPYKPMVNHAESRLNIERMKQIYQQLSRYRGLC-----LLASVPSNPNNG--GFMG	515
MmCRY1/1-606	434	PVLRGFFAKYIYDPWNAPEGIQKAKCLIGVNPYKPMVNHAESRLNIERMKQIYQQLSRYRGLC-----LLASVPSNPNNG--GFMG	515
ErCRY1/1-620	434	PVLRGFFAKYIYDPWNAPESIQKAACIIIGVNPYKPMVNHAESRLNIERMKQIYQQLSRYRGLC-----LLATVPSNPNNGNGGLMG	517
SbCRY1/1-620	434	PVLRGFFAKYIYDPWNAPESIQKAACIIIGVNPYKPMVNHAESRLNIERMKQIYQQLSRYRGLC-----LLATVPSNPNNGNGGLMG	517
GgCRY1/1-621	434	PVLRGFFAKYIYDPWNAPESVQKAACIIIGVNPYKPMVNHAESRLNIERMKQIYQQLSRYRGLC-----LLATVPSNPNNGNGGLMS	517
DpCRY2/1-742	459	PVLKMMTRYITHEPVCPEEIKSIRGIIIGKDVPMPIVDHTKASEINLERIKQVYLAQAKFKPQCALI----PQMLQRPNVLQSSFSPTSIITAN----	548
MbCRY1/1-548	448	PELARMPVEYIYEPWKAPIDIGERATCIIGKDYAPVNVHLVAAQRNK-----NAMKWLGRSVAGRLDKEKWFELVGLRHFLQKAPPHCCPSSSEDIRQF	543
HaCRY1/1-528	448	PELARMPVEYIYEPWKAPIDIGERATCIIGKDYAPVNVHLVAAQRNK-----NAMK-----ELRHMQLKAPPHCCPSSSEDIRQF	523
BmCRY1/1-536	445	PELARVTEYIYEPWKAPLDVQERANCIIGKDYAPVNVHLVAAQRNRN-----AMEDTKMEKNHAKQGRGRPLASSNSGR-----	519
DpCRY1/1-534	445	PELARMPGEYIYEPWKAPLEVDQEAAGCVIGRDYAPVDVHTAAARNRANMQ-----ELRRLLEKAPPHCCPSSSEDIRQF	520
DmCRY1/1-542	456	PELMNVKEFVHEPWRMSAEQGEQVECLIGVHYPERIDLSMAVKNMLAMKSLRNSLITP-----PPHCRPSNEEEVRQF	534
NbCRY1/1-542	459	PELANVKEYITHEPWRPMNIQEDSDCVGIHYPERIDLVNAQCKRTIARTLRNALIAEGAPDN-----GPHCRPSNEEEVRQF	537
AgCRY1/1-545	456	PELANVQAQFVHEPWKASREQIIEYGCVIIEKYPAPMVDLAVISKRNAHTMASLREKLVDDGS-----TPHCRPSDIEEIRQF	534
HeCRY2/1-593	526	-----VEDLSHPVAE-----PSSSQAGSMSSAGPRPLPS-----GPAS--P	559
MmCRY2/1-592	525	-----VEDLSHPVAE-----PGSSQAGSISNTGPRALSSGPAS-----P	558
GgCRY2/1-582	516	-----VEDLSGPVTDG-----APGQ--GSSTSTAVRLPQS--DQAS--P	548
HeCRY1/1-586	516	YS-AENIPGCSSSGS-----CSQSGGILHYAHGDSQQTHLLKQGRSSMTGLSGGKRPSQE-----EDTQSIGP	578
MmCRY1/1-606	516	YAPGENVPSCSSSGNGGLMGYPAGEN-VPSCSGGN-----CSQSGGILHYAHGDSQQTHSLKQGRSSAGTGLSSGKRPSQE-----EDAQSVGP	598
ErCRY1/1-620	518	YSPGESISGCGSTGGAQLGTGDGHTV-VQSCITLGDHSHTSGVQQQGYCQASS-ILHYAHGDNQQSHLLQAGRTALGTGISAGKRPNPPE-----EETQSVGP	612
SbCRY1/1-620	518	YSPGESISGCGSTGGAQLGAGDGHV-VQSCALGDSHTGTSGVQQQGYCQASS-ILHYAHGDNQQSHLLQAGRTALGTGISAGKRPNPPE-----EETQSVGP	612
GgCRY1/1-621	518	FSPGESISGCSAGGAQLGTGDGQTVGVQTCALGDSHTGSGVQQQGYCQASS-ILRYAHGDNQQSHLMQPGRASLTGTGISAGKRPNPPE-----EETQSVGP	613
DpCRY2/1-742	549	-----INQSNYLCQSQS--DVP TPTNQTIN-----QFKEDAVFLKP	582
MbCRY1/1-548	544	MWLNE-----	548
HaCRY1/1-528	524	MWLNE-----	528
BmCRY1/1-536	520	RWNSPLDYQQTGREKIY-----	536
DpCRY1/1-534	521	MWLGDSSQPELTTT-----	534
DmCRY1/1-542	535	FWLADVIV-----	542
NbCRY1/1-542	538	FWLAD-----	542
AgCRY1/1-545	535	FWLADDAATEA-----	545
HeCRY2/1-593	560	KRKLEAAEPPGEELSKRARVAELPTPELPSKDA-----	593
MmCRY2/1-592	559	KRKLEAAEPPGEELTKRARVTEMPTQEPASKDS-----	592
GgCRY2/1-582	549	KRKHEGAELCTEELYKRAKVTGLPAPEIPGKSS-----	582
HeCRY1/1-586	579	KVQRQSTN-----	586
MmCRY1/1-606	599	KVQRQSSN-----	606
ErCRY1/1-620	613	KVQRQSTN-----	620
SbCRY1/1-620	613	KVQRQSTN-----	620
GgCRY1/1-621	614	KVQRQSTN-----	621
DpCRY2/1-742	583	TVNNIKSNVDKQQKQVQVIVQEDKHSENQRHSVGNKYIVNEINKNINDIPVKQNNYDFKALTNLNKFNSNEPLTFLNQTPNKNESFGQDVNNVIDVYST	682
MbCRY1/1-548	549	-----	548
HaCRY1/1-528	529	-----	528
BmCRY1/1-536	537	-----	536
DpCRY1/1-534	535	-----	534
DmCRY1/1-542	543	-----	542
NbCRY1/1-542	543	-----	542
AgCRY1/1-545	546	-----	545

Figure S11 (continued). Sequence alignment of Type I and Type II CRY (part 2).

HsCRY2/1-593	594	-----	593
MmCRY2/1-592	593	-----	592
GgCRY2/1-582	583	-----	582
HsCRY1/1-586	587	-----	586
MmCRY1/1-606	607	-----	606
ErCRY1/1-620	621	-----	620
SbCRY1/1-620	621	-----	620
GgCRY1/1-621	622	-----	621
<hr/>			
DpCRY2/1-742	683	SKPKFYFTDNGVITHNENAQTFKRDSYSDNYNKESTGSNRVGEVHSNNPQTDKISSEKKN	742
MbCRY1/1-548	549	-----	548
HaCRY1/1-528	529	-----	528
BmCRY1/1-536	537	-----	536
DpCRY1/1-534	535	-----	534
DmCRY1/1-542	543	-----	542
NbCRY1/1-542	543	-----	542
AgCRY1/1-545	546	-----	545

Figure S11 (continued). Sequence alignment of Type I and Type II CRY (part 3). Sequence alignment between eight Type I and eight Type II CRY. Colour coding: The darker the underlying blue the higher the sequence similarity within the chosen sixteen sequences. Abbreviations: Hs = *Homo sapiens* (human), Mm = *Mus musculus* (house mouse), Gg = *Gallus gallus* (chicken), Er = *Erithacus rubecula* (European robin), Sb = *Sylvia borin* (garden warbler), Dp = *Danaus plexippus* (monarch butterfly), Mb = *Mamestra brassicae* (cabbage moth), Ha = *Helicoverpa armigera* (cotton bollworm), Bm = *Bombyx mori* (domesticated silkworm), Dm = *Drosophila melanogaster* (fruit fly), Nb = *Neobellieria bullata* (grey flesh fly), Ag = *Anopheles gambiae* (mosquito).

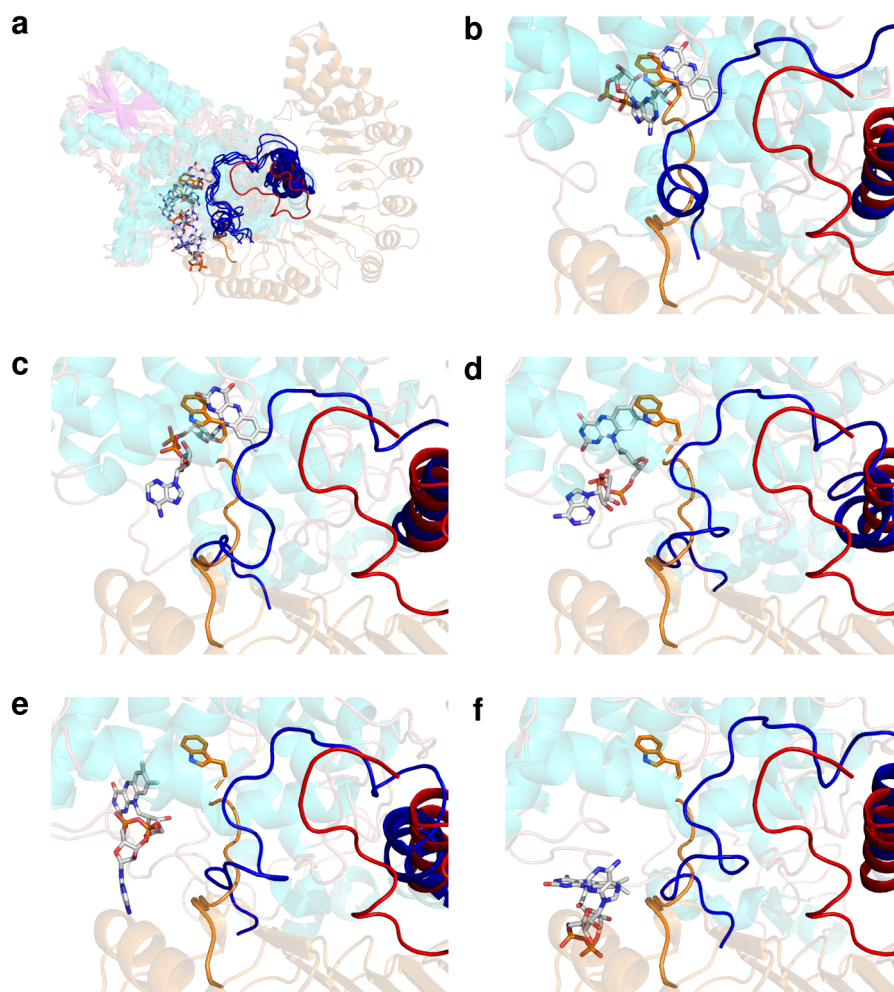


Figure S12. Comparison between MmCRY2 structures from metadynamics simulations with the MmCRY2/FBLX3-Complex. **a:** Overlay between the MmCRY2/FBLX3-complex (PDB code: 4I6J; 7 amino acids at the C-terminus are not resolved) with the five snapshots (**b-f**) from the metadynamics simulations at M0 to M4 from Figure 2 (58 amino acids are missing in our model since these are not resolved). **b-f:** Zoom of the FAD-binding pocket for each individual snapshot M0 (**b**) to M4 (**f**). Colour coding: FBXL3: orange; C-terminus of FBXL3: red; MmCRY2: cyan; C-terminus of MmCRY2: blue; FAD: highlighted with white carbon atoms.

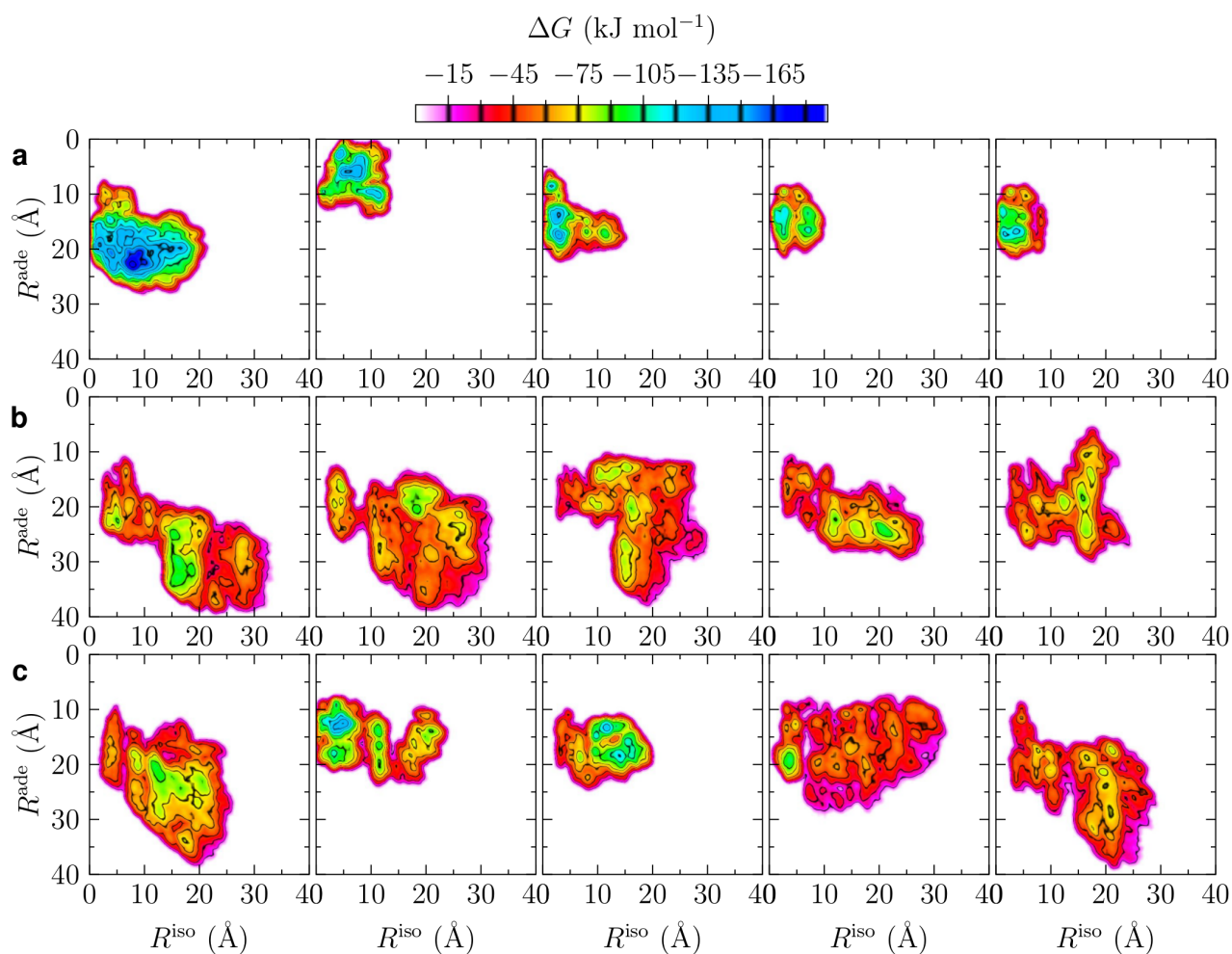


Figure S13. FAD-binding studies based on metadynamics simulations. Five individual 2-dimensional free energy (ΔG) plots for FAD (un)binding from 100 ns MTD simulations for each of DmCRY (**a**), MmCRY2 (**b**) and SbCRY1a (**c**). R^{ade} is the distance between the centre-of-masses of the adenine and the binding pocket residues, and R^{iso} the distance between the centre-of-masses of the isoalloxazine and the binding pocket residues as shown in Figure S4.

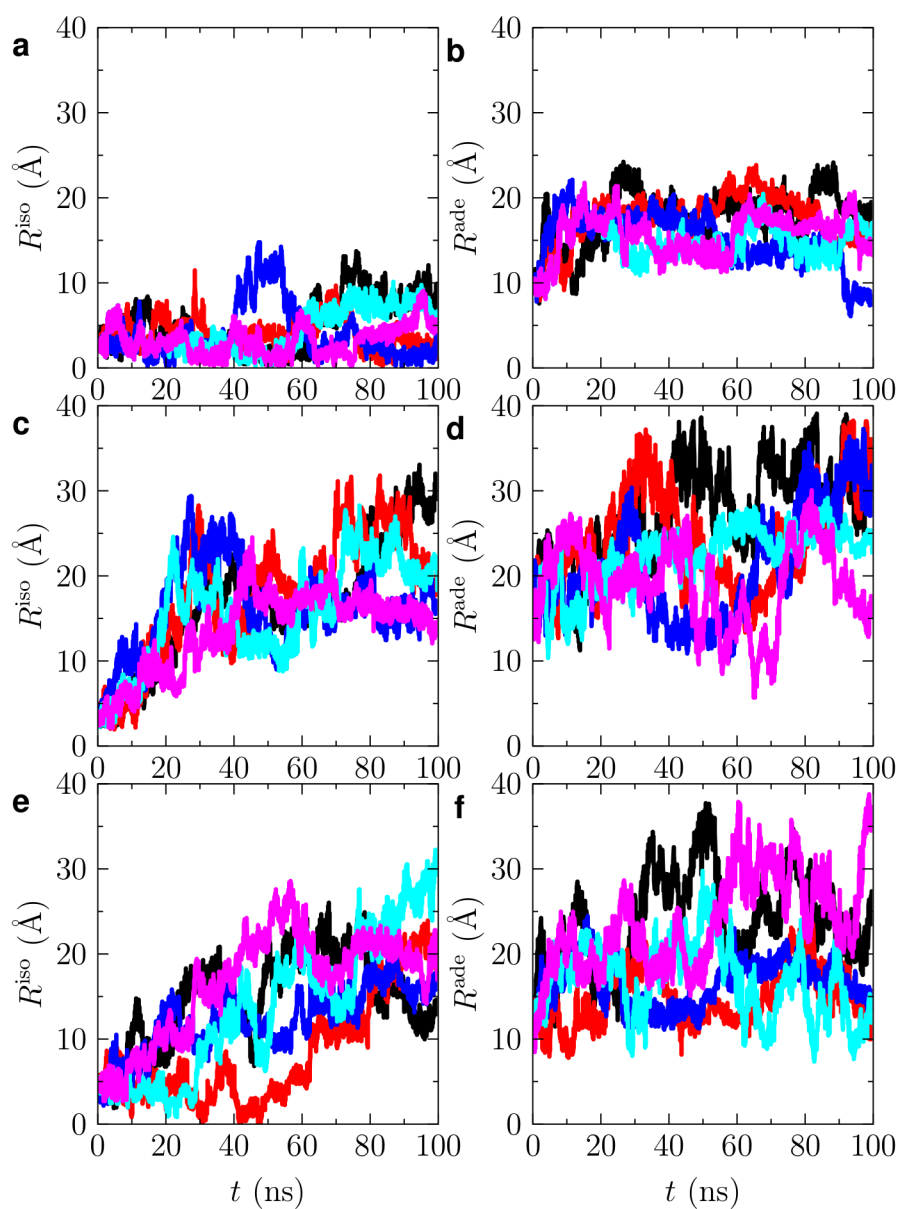


Figure S14. FAD-binding studies based on metadynamics simulations. Plotted are the values of the CVs, R^{iso} and R^{ade} , for each individual of five simulations over 100 ns for the systems DmCRY (a and b), MmCRY2 (c and d), and SbCRY1a (e and f).

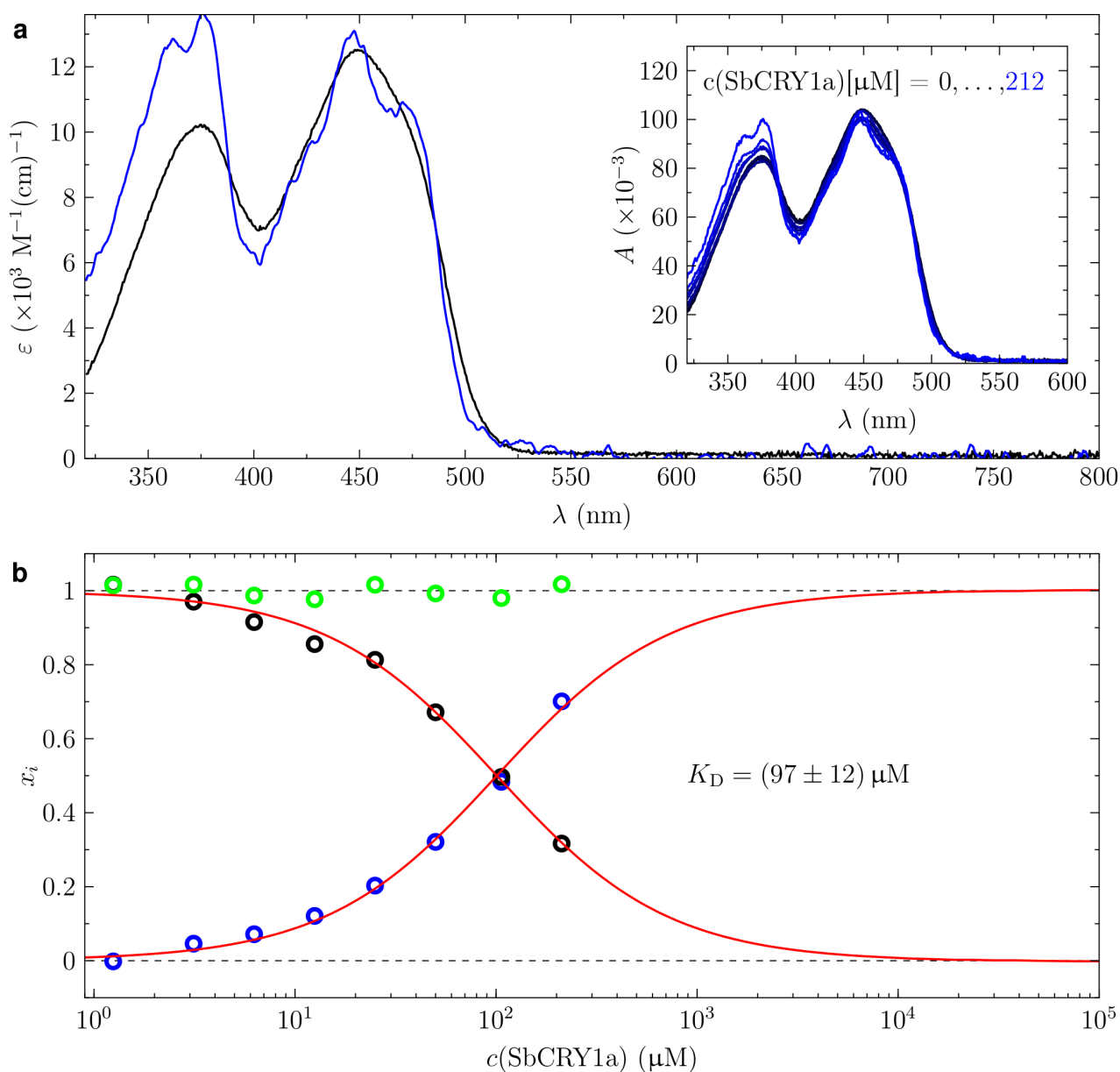


Figure S15. Determination of the FAD-binding affinity in SbCRY1a. **a:** pure UV-visible absorption spectra of unbound FAD (black) and bound in SbCRY1a (blue) extracted from the raw data (inset in panel **a**: raw data minus fitted scatter contribution) as described in the Materials and Methods section of the main text. **c:** mole fractions of unbound FAD (black open circles) and bound in SbCRY1a (blue open circles) as determined from fitting the pure spectra from panel **a** to each spectrum of the inset in panel **a** correlated with the SbCRY1a-apo concentration. The green open circles represent the sum of the mole fractions. The red lines represent the global fits of the binding equation 4 to the data.

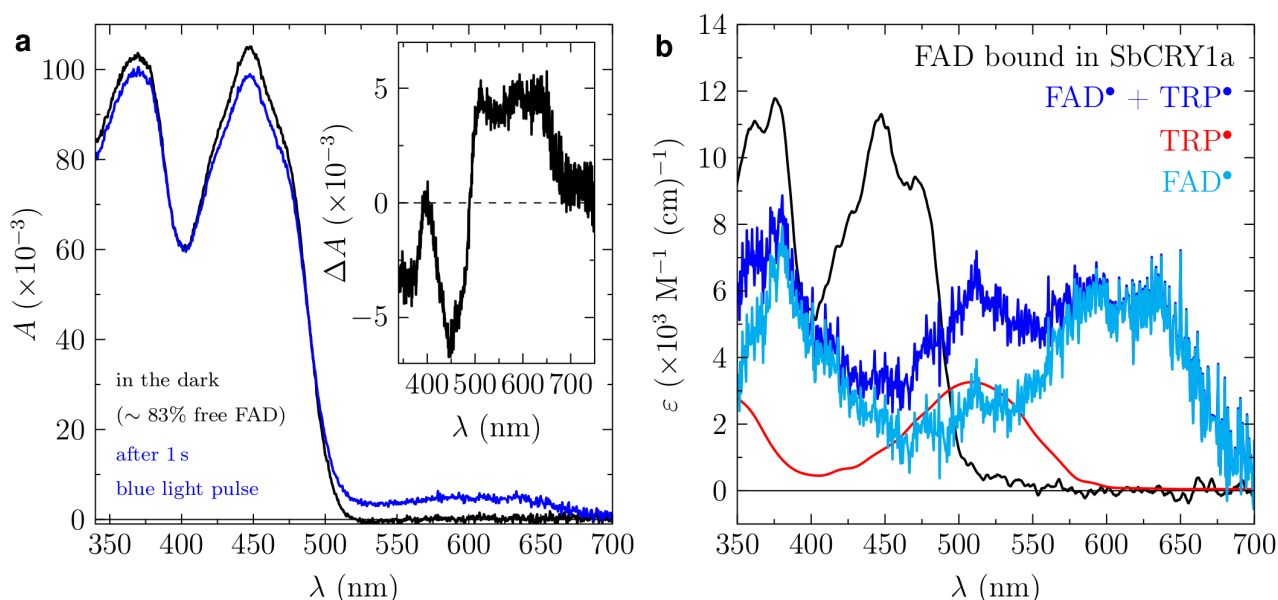


Figure S16. Determination of the pure neutral FAD radical spectrum and the counter neutral tryptophan radical in SbCRY1a via *in silico* titration. Absorption spectra of a sample containing 8 μM FAD and *ca.* 33.8 μM SbCRY1a before (black line in panel **a**) and directly after illumination with a 1 s blue-light pulse (blue line in panel **a**). Since this sample still contained *ca.* 13% of unbound FAD, the difference spectrum (inset in panel **a**) subtracts the contribution of unbound FAD. Adding the pure spectrum of fully bound FAD to SbCRY1a from Figure S15a to the difference spectrum in such a way that its characteristic fine structural features disappear, results in a spectrum (blue line in panel **b**) with a high similarity to known spectra for the neutral flavin semiquinone radical, *e.g.* shown in^{1,2}. However, some deviations can still be seen especially in the range between 450 to 550 nm. These deviations can be explained by the contributions of the neutral tryptophan radical (red line extracted from³). By subtracting a certain amount of the neutral tryptophan radical from the mixture spectrum it is possible to obtain a perfect match to the known flavin neutral radical spectrum (cyan line). (A detailed time-resolved analysis of the mechanism including branching ratios, the photoproduct, and a discussion about the proton donor is beyond the scope of this work and will be presented elsewhere.)

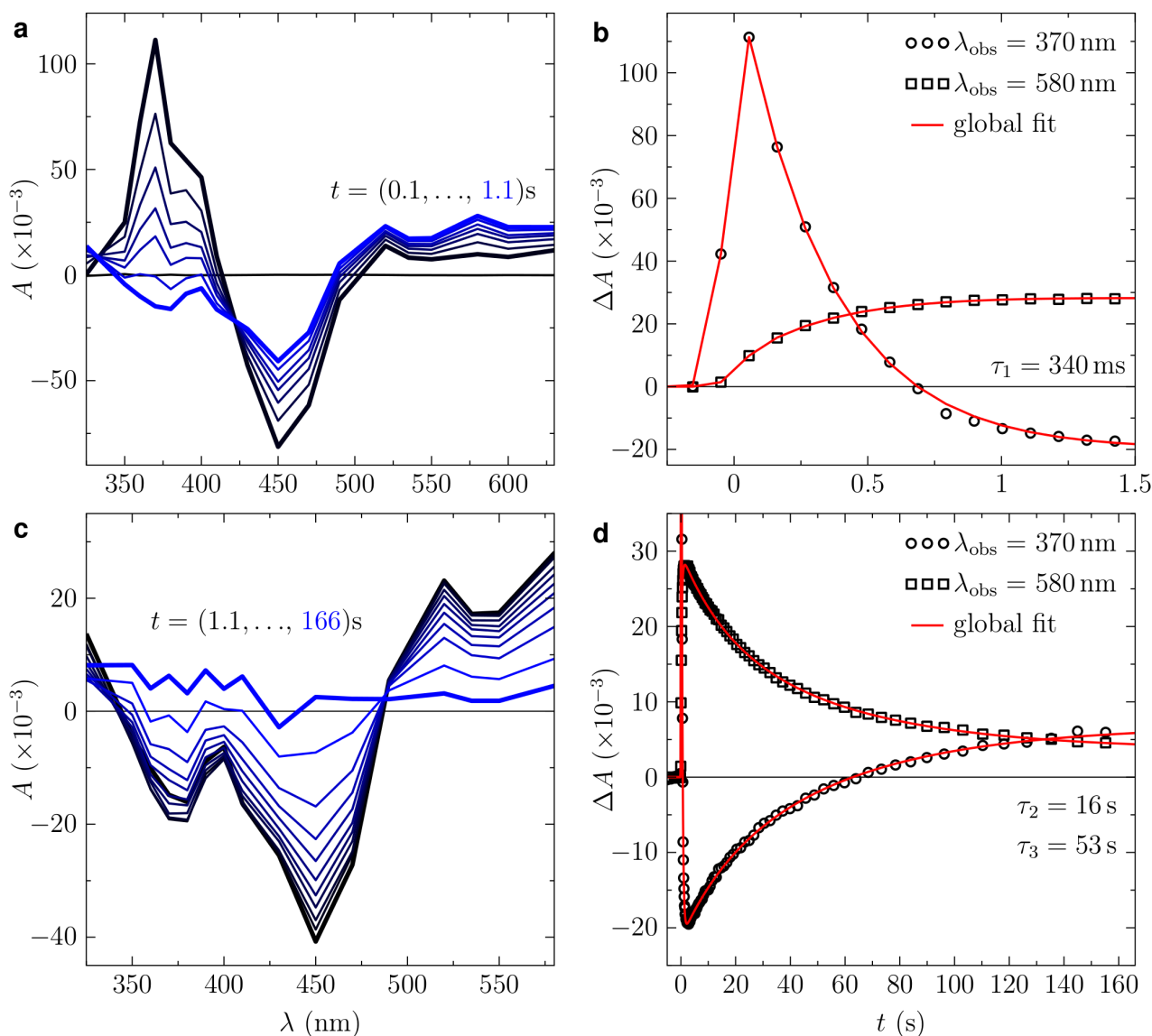


Figure S17. Photo-induced formation and decay of the neutral FAD semiquinone radical bound in SbCRY1a. UV-visible absorption changes at single wavelengths in the range from 350 to 580 nm induced by single 100 ms blue-light pulse were recorded a sample containing 27.4 μM FAD and *ca.* 690 μM SbCRY1a. The spectrally (**a** and **c**) and temporally (**b** and **d**) resolved UV-visible absorption changes up to 1 s (**a** and **b**) and 160 s (**c** and **d**) are shown at two selected wavelength representative for the main features of the anionic (370 nm) and neutral (580 nm) FAD semiquinone radicals. The red lines represent the global fit of two exponential functions to the entire data matrix with the lifetimes of 340 ms, 16 s, and 53 s. (A detailed time-resolved analysis of the mechanism including branching ratios, the photoproduct, and a discussion about the proton donor is beyond the scope of this work and will be presented elsewhere.)

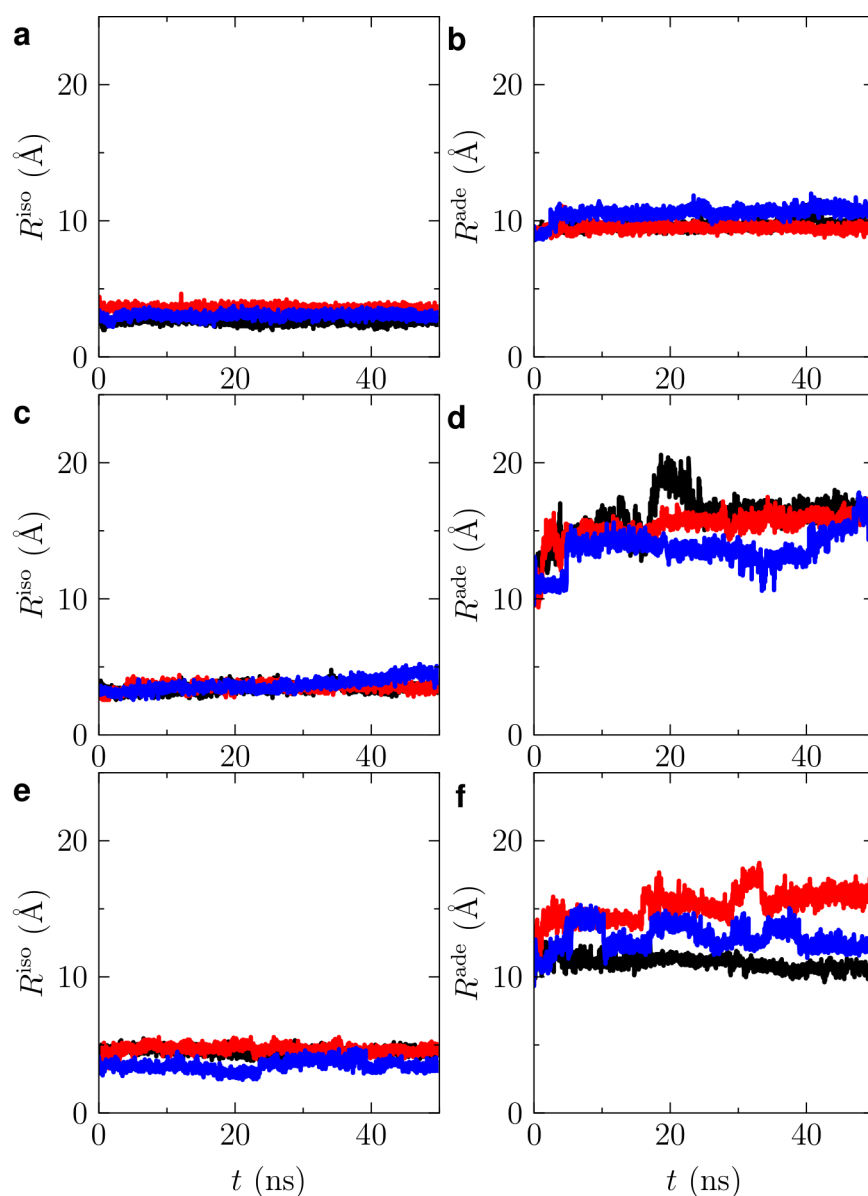


Figure S18. Movement of FAD during conventional MD simulations. Plots of R^{iso} and R^{ade} for DmCRY (a,b), MmCRY2 (c,d) and SbCRY1a (e,f) from 3 MD simulations using different seeds for initial velocity generation. While the FAD remains bound during each of these short simulations, the adenine is clearly more tightly bound in DmCRY, in accord with the structural differences outlined in Figure 3.

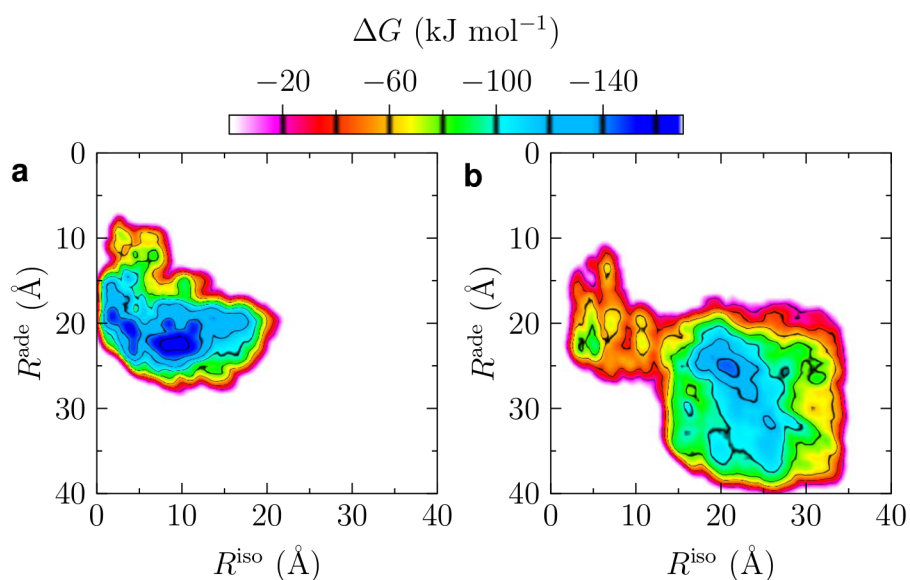


Figure S19. FAD-binding studies based on metadynamics simulations. 2-dimensional free energy (ΔG) plots for FAD (un)binding from 300 ns MTD simulations for DmCRY (a) and MmCRY2 (b). R^{ade} is the distance between the centre-of-masses of the adenine and the binding pocket residues, and R^{iso} the distance between the centre-of-masses of the isoalloxazine and the binding pocket residues as shown in Figure S9.

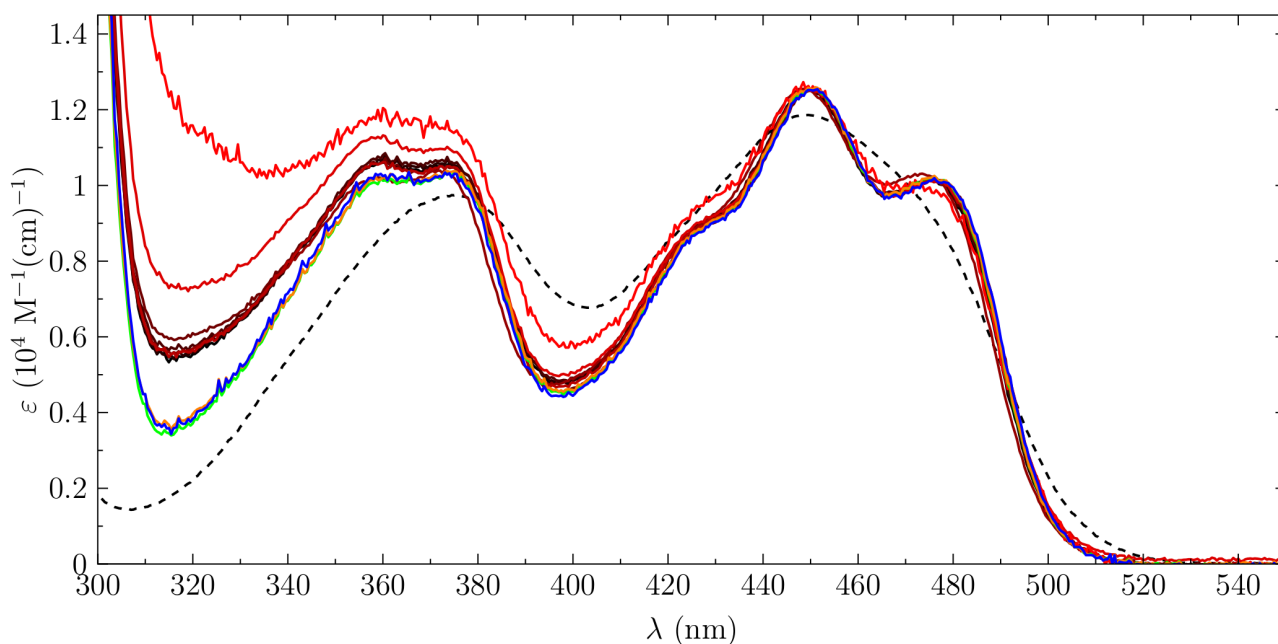


Figure S20. UV-visible absorption of DmCRY wild type, variants and free FAD. Zoom of Figure 3c in the spectral range from 300 to 550 nm. The colour coding corresponds to the inset in Figure 3c. The additional colours correspond to spectra of the following mutants: Q311A (green), R298Q-Q311A (orange), and R237Q-Q311A (blue). The extinction coefficients are scaled to the absorbance maximum of FAD at 450 nm. The additional variants resulted in no effect for the single variant, but in a loss in FAD binding affinity at maximum for the variant R237Q-Q311A, of ca. 8%. The small effect can be explained most likely due to the H-bonding ability of the glutamine, which somewhat restores – not to the same extent as the wild type – the interaction to the FAD pyrophosphate. However, this variant does not introduce new electrostatic interactions and, thus, a disruption of the whole protein structural conformation is less likely demonstrating the importance of the discussed amino acids necessary for FAD binding. Since these variants as well as the double variant R298E-Q311E show almost identical fine structures in their UV/Vis absorption spectra due to bound FAD, one can assume that the interaction site for the isoalloxazine ring is comparable/identical to wild type.

References

1. Kutta, R. J., Kensy, U. & Dick, B. Measuring photochemical intermediates with a streak camera - a new technique for transient absorption. in *Chemical Photocatalysis* (2013).
2. Lanzl, K., Sanden-Flohe, M. v., Kutta, R. J. & Dick, B. Photoreaction of mutated LOV photoreceptor domains from *chlamydomonas reinhardtii* with aliphatic mercaptans: implications for the mechanism of wild type LOV. *PCCP* **12**, 6594–6604 (2010).
3. Solar, S., Getoff, N., Surdhar, P. S., Armstrong, D. A. & Singh, A. Oxidation of tryptophan and N-methylindole by N_3^\bullet , Br_2^- , and $(\text{SCN})_2^-$ radicals in light- and heavy-water solutions: a pulse radiolysis study. *J. Phys. Chem.* **95**, 3639–3643 (1991).

